doi:10.1093/brain/awz025 BRAIN 2019: 142; 1148–1160 | 1148

BRAIN
A JOURNAL OF NEUROLOGY

Entorhinal cortex tau, amyloid-β, cortical thickness and memory performance in non-demented subjects

David S. Knopman,[1] Emily S. Lundt,[2] Terry M. Therneau,[2] Prashanthi Vemuri,[3] Val J. Lowe,[3] Kejal Kantarci,[3] Jeffrey L. Gunter,[3] Matthew L. Senjem,[3] Michelle M. Mielke,[2] Mary M. Machulda,[4] Bradley F. Boeve,[1] David T. Jones,[1] Jon Graff-Radford,[1] Sabrina M. Albertson,[2] Christopher G. Schwarz,[3] Ronald C. Petersen[1] and Clifford R. Jack Jr.[3]

As more biomarkers for Alzheimer's disease and age-related brain conditions become available, more sophisticated analytic approaches are needed to take full advantage of the information they convey. Most work has been done using categorical approaches but the joint relationships of tau PET, amyloid PET and cortical thickness in their continuous distributions to cognition have been under-explored. We evaluated non-demented subjects over age 50 years in the Mayo Clinic Study of Aging, 2037 of whom had undergone 3 T MRI scan, 985 amyloid PET scan with ^{11}C-Pittsburgh compound B (PIB) and MRI, and 577 PIB-PET, ^{18}F-AV1451 flortaucipir PET and MRI. Participants received a nine-test cognitive battery. Three test scores (logical memory delayed recall, visual reproduction delayed recall and auditory verbal learning test delayed recall) were used to generate a memory composite z-score. We used Gradient Boosting Machine models to analyse the relationship between regional cortical thickness, flortaucipir PET signal, PIB-PET signal and memory z-scores. Age, education, sex and number of test exposures were included in the model as covariates. In this population-based study of non-demented subjects, most of the associations between biomarkers and memory z-scores accrued after 70 years of age. Entorhinal cortex exhibited the strongest associations between biomarkers and memory z-scores. Other temporal regions showed similar but attenuated associations, and non-temporal regions had negligible associations between memory z-scores and biomarkers. Entorhinal flortaucipir PET signal, PIB-PET signal and entorhinal cortical thickness were independently and additively associated with declining memory z-scores. In contrast to global PIB-PET signal where only very high amyloid-β levels were associated low memory z-scores, entorhinal flortaucipir PET signal just above background levels was associated with low memory z-scores. The lowest memory z-scores occurred with the confluence of elevated entorhinal flortaucipir PET signal and lower entorhinal cortical thickness.

1 Department of Neurology, Mayo Clinic, Rochester, MN, USA
2 Department of Health Sciences Research, Mayo Clinic, Rochester, MN, USA
3 Department of Radiology, Mayo Clinic, Rochester, MN, USA
4 Department of Psychiatry and Psychology, Mayo Clinic, Rochester, MN, USA

Correspondence to: David Knopman, MD
Department of Neurology, Mayo Clinic, Rochester MN 55905 USA
E-mail: knopman@mayo.edu

Keywords: amyloid PET; flortaucipir PET; cortical thickness, memory

Abbreviations: GBM = gradient boosting machine; MCSA = Mayo Clinic Study of Aging; PIB = Pittsburgh compound B; SUVR = standardized uptake value ratio

Received October 3, 2018. Revised December 3, 2018. Accepted December 15, 2018. Advance Access publication February 12, 2019

Introduction

The confluence of β-amyloidosis, tauopathy, and synaptic and neuronal loss/dysfunction often culminates in the cognitive disorder of Alzheimer's disease. Studying the cognitive consequences of any one of these processes individually through their biomarker proxies is tractable. Examining the continuous distributions of more than one biomarker simultaneously becomes particularly challenging. Most prior work studying cognitive outcomes as a function of multiple biomarkers has resorted to dichotomizing the biomarkers as normal or abnormal (Burnham *et al.*, 2016; Jack *et al.*, 2016; Bilgel *et al.*, 2018; Lowe *et al.*, submitted for publication). There are many practical and analytic advantages to categorical groupings, but there are limitations. A categorical approach depends on the assumption that biomarker biology can be faithfully represented by step functions. It is much more likely that relationships between biomarker levels and cognition are more complex.

Working initially with Pittsburgh compound B (PIB) for β-amyloidosis and cortical thickness measures from 3 T structural MRI as a neurodegeneration biomarker, we adapted an analytic approach, Gradient Boosting Machine (GBM), to model the associations of cognition with the continuous distributions of multiple biomarkers in participants in the Mayo Clinic Study of Aging (MCSA) (Knopman *et al.*, 2018). We chose the GBM approach because it was best-suited to deal with the non-normal distributions and non-linearity of relationships between cognition and biomarkers. As we have subsequently imaged a sufficiently large enough group of individuals who have also had ^{18}F-AV1451 flortaucipir, we sought to model simultaneously all three imaging biomarkers in relation to cognition. Our goal was to understand the relationships between the three biomarkers and cognition in asymptomatic and mildly symptomatic, non-demented people.

Materials and methods

Participants

This analysis was based on residents aged $\geqslant$50 years of Olmsted County Minnesota who were imaged in the MCSA between 2009 and 2018. Participants were non-demented (either cognitively unimpaired or mild cognitive impairment) as determined by diagnostic procedures described previously (Petersen 2004, 2010; Roberts *et al.*, 2008, 2012, 2014), which included an examination by a physician, a cognitive battery and an interview of participant and informant by a study coordinator in order to complete a Clinical Dementia Rating. There were generally equal numbers of males and females, by design. With the exception of subjects with contraindications to MRI scanning, all MCSA participants were invited to undergo imaging.

For reference purposes, we also present a group of 83 subjects enrolled in the MCSA or Mayo Alzheimer's Disease Research Center (mean age 78, range 70–92; 36 female) with a clinical diagnosis of Alzheimer dementia who had elevated amyloid-β on PIB.

Standard protocol approvals, registrations, and patient consents

This study was approved by the Mayo Clinic and Olmsted Medical Center Institutional Review Boards. All participants provided written consent in accordance with the Mayo Clinic Foundation and Olmsted Medical Center Institutional Review Boards. All potential conflicts of interest and sources of funding are disclosed herein.

Cognitive outcome measures

All MCSA participants undergo a nine-test cognitive battery that has been described previously (Roberts *et al.*, 2008; Knopman *et al.*, 2015). The primary outcome measure in this analysis was a memory domain z-score. Three tests [logical memory delayed recall, visual reproduction delayed recall and auditory verbal learning test (AVLT) delayed recall] were used to quantitate delayed recall. Individual test scores were converted to z-scores based on a reference cohort of clinically normal MCSA participants ages 50–89 years enrolled between 2004 and 2012, and weighted to the Olmsted County MN population. The score was adjusted for number of prior neuropsychological testing sessions. A global z-score was also generated from all nine cognitive tests, and was used in sensitivity analyses.

Imaging

Among cognitively unimpaired participants, 2037 had undergone 3 T MRI scan, of whom 985 had undergone PIB and MRI, and 577 who had undergone PIB, flortaucipir and MRI scanning. Among those with mild cognitive impairment who had a 3 T MRI (n = 210), there were 103 who had undergone PIB and MRI, and 25 who had undergone PIB, flortaucipir and MRI scanning. Time of introduction of the scanning modality accounted for the differences in numbers of participants with the three scans, MRI first, PIB second and flortaucipir last.

MRI acquisition

We used cortical thickness as the measure of cortical structural integrity. As described in detail elsewhere (Schwarz *et al.*, 2016), regional cortical thickness was estimated from magnetization-prepared rapid-acquisition gradient echo (MPRAGE) sequences performed on 3 T MRI scanners (General Electric Healthcare) with an eight channel phased array head coil. Sequences were processed through an SPM12 (Ashburner *et al.*, 2005) pipeline using Mayo Clinic Adult Lifespan Template (MCALT; https://www.nitrc.org/projects/mcalt/) (Schwarz *et al.*, 2017) tissue priors and settings optimized for our study population. Cortical thickness measurements were then calculated from the resulting tissue-class segmentations using DiReCT (Das *et al.*, 2009). Regions of interest were defined on each MRI by transforming the MCALT_ADIR122 atlas using Advanced Normalization Tools (ANTs) (Avants *et al.*, 2008). These T_1-weighted 3D

high-resolution scans were also used for anatomical segmentation and labelling of PET images.

PET acquisition

Tau PET was performed using the ^{18}F-AV-1451 (flortaucipir) ligand and amyloid-β PET was performed using the ^{11}C-PiB ligand on a PET/CT scanner (GE Healthcare) operating in 3D mode as previously described (Schwarz *et al.*, 2016; Jack *et al.*, 2017, 2018; Vemuri *et al.*, 2017; Lowe *et al.*, 2018). For flortaucipir PET, an intravenous bolus injection of ~370 MBq (range 330–406 MBq) was administered, followed by an 80-min uptake period, and a 20-min scan acquisition. For PIB, an injection of ~627 MBq (range 384–722 MBq) of PIB was administered, followed by a 40-min uptake period, and a 20-min PIB scan of four 5-min dynamic frames. An automated image processing pipeline for PET image analysis included rigid registration of the PET volumes to each patient's own T_1-weighted MRI for the segmentation of grey and white matter. Regions of interest were defined using the transformed MCALT_ADIR122 atlas, masked to include only those voxels labelled primarily as grey or white matter.

Regional ^{11}C-PIB uptake was defined as the median uptake across all voxels in a region of interest. We also defined a global PIB standardized uptake value ratio (SUVR) calculated from the region-size weighted average of grey plus white matter in bilateral parietal (including posterior cingulate and precuneus), orbitofrontal, prefrontal, temporal, and anterior cingulate regions, referenced to the right and left cerebellar crus grey matter. No partial volume correction was used. This meta-region of interest was based on our prior work (Jack *et al.*, 2008), and has been validated neuropathologically (Murray *et al.*, 2015). We will refer to ^{11}C-PIB binding as PIB SUVR hereafter.

We examined global PIB SUVR as our primary measure of brain amyloidosis because amyloid-β plaque pathology is present in a widespread fashion by the time it reaches nominal clinical cut-point levels (Grothe *et al.*, 2017), and local levels are closely correlated with global level (Lockhart *et al.*, 2017). We also conducted analyses using regional PIB SUVR and re-examined associations with cognition.

Flortaucipir uptake in each region of interest was divided by the median value of the right and left cerebellar crus uptake. No partial volume correction was used. Regional flortaucipir SUVR was determined for combined right and left hemispheres in 46 regions. Based on our prior work with flortaucipir in cognitively unimpaired subjects (Lowe *et al.*, submitted for publication) in which entorhinal cortex showed the strongest associations with categorical elevated PIB and elevated flortaucipir, we focused on this region. We also examined other regions (Lowe *et al.*, 2018) including two other temporal regions of interest, and two regions of interest that had much lower tau levels in non-demented individuals and were less associated with memory, posterior cingulate and prefrontal (frontal inferior operculum, inferior orbital frontal, medial orbital frontal, mid frontal, mid orbital frontal, superior frontal, superior orbital frontal). See Supplementary Fig. 1 for regional flortaucipir SUVR values in cognitively unimpaired subjects.

Analysis

We explored the relationships between regional cortical thickness, tau SUVR and PIB SUVR for predicting memory z-scores using a machine learning model, GBM as described previously for this purpose (Knopman *et al.*, 2018). Models were fit in each of the five regions of interest. Age, education and sex were included as covariates and an interaction depth of two was specified allowing for all possible 2-way interactions. To account for learning effect due to exposure to the neuropsychological test battery prior to the visit at which the current imaging data were collected, we used the entire MCSA cohort to estimate the learning effect over repeated exposures to the cognitive battery using a linear mixed effects model. The estimated effect (0.26, 0.36, 0.44) for having taken the cognitive battery (two, three, four or more) times, respectively, were subtracted from the memory z-score. The GBM model accommodates missing data so that we chose to include participants who had undergone only MRI or only MRI and PIB to take advantage of their larger numbers for refining estimates derived from the model. The model complexity (number of subtrees) was chosen using 8-fold cross-validation.

We predicted the marginal effects of flortaucipir SUVR, PIB SUVR, cortical thickness, and age over the covariates of education and sex. For flortaucipir SUVR, PIB SUVR and cortical thickness, the maximum and minimum by decade were observed to have occasional extreme values. Because the GBM model returns a flat line in regions where there are no data, we added limits based on 3rd and 97th percentile values by decade and region in order to declutter the heat maps and 2D plots. The 3D heat maps displayed imaging values on the *x*- and *y*-axes and memory (or global) z-scores as a colour code to represent the *z*-axis. The 2D figures displayed an imaging feature on the *x*-axis and memory z-scores on the *y*-axis with a family of cubic smoothing spline curves representing different discrete values of the other imaging feature. For consistency with the other two biomarkers, the scale for cortical thickness is inverted for all heat maps. Thus, more abnormal values are always to the right on the *x*-axis or upward on the *y*-axis.

Analyses were performed in R statistical software version 3.4.2 (R Core Team, R Foundation of Statistical Computing, Vienna) using the GBM package version 2.1.

Confidence limits cannot be obtained directly from GBM models at this time. Bootstrapping is a non-parametric method for computing standard errors and confidence intervals. For each of 1000 replicates we resampled the data with replacement fitting new GBM models to each sample, and summarize differences and standard errors. We tabulated differences between the 5th and 95th percentiles of biomarker values as shown in the 2D figures.

Data availability

The Mayo Clinic Study of Aging makes data available to qualified researchers upon reasonable request.

Results

Table **1** shows the demographics and basic descriptive statistics on imaging features in the study group. The group ranged in age from 50 and 90 years, with few >90 years old. Memory z-scores generally declined with age but there was wide variability (Supplementary Fig. 1).

Table 1 Demographics and PIB SUVR values of study participants

Feature	Overall (*n* = 2247)	Group with MRI only (*n* = 557)	Group with MRI + PIB-PET (*n* = 1088)	Group with MRI + PIB-PET + flortaucipir PET (*n* = 602)
Age in years (%)				
50–59	280 (12.5)	19 (3.4)	144 (13.2)	117 (19.4)
60–69	501 (22.3)	30 (5.4)	290 (26.7)	181 (30.1)
70–79	770 (34.3)	232 (41.7)	374 (34.4)	164 (27.2)
80–89	636 (28.3)	251 (45.1)	257 (23.6)	128 (21.3)
90 +	60 (2.7)	25 (4.5)	23 (2.1)	12 (2.0)
Female, *n* (%)	1085 (48.3)	297 (53.3)	521 (47.9)	267 (44.4)
Education, years				
Mean (SD)	14.6 (2.66)	14.0 (2.73)	14.6 (2.72)	14.9 (2.42)
Quartile 1, Quartile 3	12, 16	12, 16	12, 16	13, 16
Cognitive status				
Cognitively unimpaired	2037	475	985	577
Mild cognitive impairment	210	82	103	25
***APOE* ε4 carrier (%)**	635 (28.6)	161 (29.1)	301 (27.8)	173 (29.4)
Short test of mental status score (max = 38)				
Mean (SD)	34.8 (2.76)	33.7 (2.92)	34.8 (2.73)	35.7 (2.26)
Quartile 1, Quartile 3	33, 37	32, 36	33, 37	35, 37
Range	22–38	24–38	22–38	22–38
Prior exposure to cognitive tests, *n* (%)				
0	698 (31.1)	171 (30.7)	508 (46.7)	19 (3.2)
1	338 (15)	53 (9.5)	216 (19.9)	69 (11.5)
2 +	1211 (53.9)	333 (59.8)	364 (33.5)	514 (85.4)
Global PIB SUVR				
Mean (SD)	1.54 (0.373)	NA	1.54 (0.375)	1.55 (0.369)
Quartile 1, Quartile 3	1.33, 1.57	NA	1.32, 1.58	1.34, 1.56
Range	1.04–3.49	NA	1.04–3.49	1.14–3.32

The entorhinal cortex was not among the regions with the highest flortaucipir SUVRs across all cortical regions (Supplementary Fig. 2), but was the region with the greatest difference in flortaucipir SUVR between those with elevated versus not elevated global PIB SUVR (cut-point = 1.48) (estimate, after adjusting for age = 0.078, $P < 0.001$) (Supplementary Fig. 3). Entorhinal cortex had the lowest regional PIB SUVR of the five regions we focused on (Supplementary Fig. 3). Differences in cortical thickness across the five regions of interest also varied as a function of elevated versus not elevated PIB SUVR (Supplementary Fig. 3). After adjusting for age, there was no difference in cortical thickness in entorhinal cortex between those with elevated versus not elevated PIB SUVR (estimate = 0.059, $P = 0.11$). Flortaucipir SUVR and cortical thickness in entorhinal cortex were modestly correlated (rho = −0.30, $P = 0.0022$) in participants in the 80–89 year old group, and uncorrelated in the younger groups (Supplementary Fig. 4).

In the GBM model, age and education had large effects on memory z-score, and females on average performed better than males (Supplementary Fig. 5).

We first show 3D heat maps for flortaucipir SUVR and cortical thickness, and will include PIB SUVR subsequently. Figure 1 presents the GBM models for memory z-score (*z*-axis, colour-coded) with regional flortaucipir SUVR (*x*-axis) and regional cortical thickness (*y*-axis) in the four age decades for all age regions. The range of values for the biomarkers has been truncated to the 3rd and 97th percentiles because the GBM model lacks sufficient data points to construct associations outside of that range; hence the coloured areas reflect the age-specific distributions of the biomarkers. The entorhinal cortex (Fig. 1A), as expected, showed the strongest relationships between memory z-scores and the two imaging biomarkers. Similar relationships (Fig. 1B–E) can be seen in the other two temporal regions of interest. In the two extra-temporal regions of interest the relationships between memory z-score and biomarkers were further attenuated.

Figure 1A illustrates three important observations about relationships between biomarkers and memory z-scores in the entorhinal cortex. First, the distribution of memory z-scores, as well as entorhinal cortex flortaucipir SUVR and entorhinal cortex cortical thickness were limited to less abnormal values in the younger age decades. With advancing age, the distributions of memory z-scores, cortical thickness and flortaucipir SUVR spanned a broader range. Second, in the oldest two groups, there was a distinct decline in memory z-scores associated within a narrow segment of the entorhinal cortex flortaucipir SUVR and entorhinal

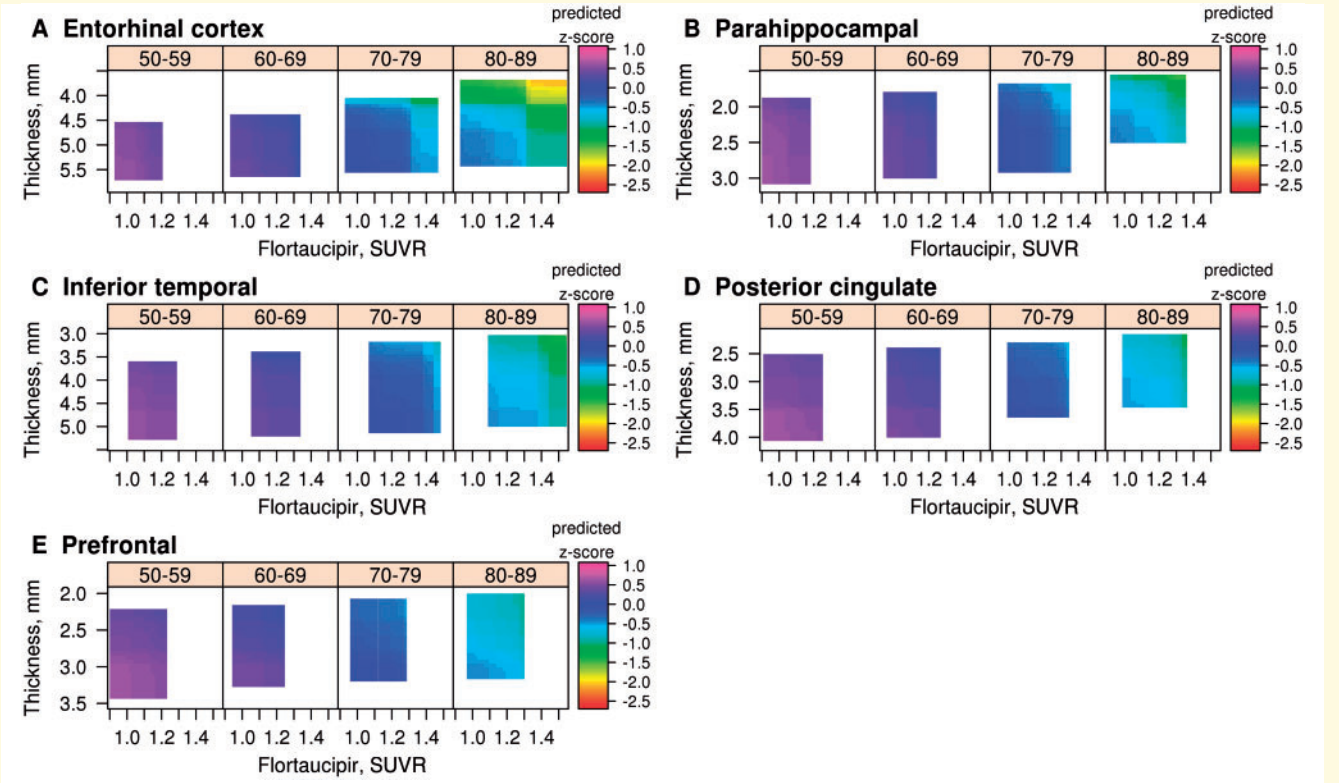

Figure 1 3D heat maps generated by GBM. (**A**) Entorhinal cortex; (**B**) parahippocampal gyrus; (**C**) inferior temporal cortex; (**D**) posterior cingulate; and (**E**) the prefrontal region of interest. For each heat map, four age ranges are represented: 50–59, 60–69, 70–79 and 80–89 years. Flortaucipir SUVR is on the *x*-axis, cortical thickness (inverted scale) on the *y*-axis and predicted memory z-score on the z-axis as depicted by the colour code for each individual graph. Heat map ranges are set at the 3rd and 97th percentiles of the distribution of each biomarker by decade of age. The key findings are that the entorhinal cortex shows the strongest associations between the biomarkers and memory z-score.

cortex cortical thickness range. These impressions are borne out in the 2D renditions in Fig. 2A and B. Over the course of 1000 replications of the model, almost all of the differences in the regional flortaucipir SUVR and cortical thickness versus memory z-scores at their 5th percentile versus 95th percentile were significant (Supplementary Table 1). Third, because interaction terms were included in the model, we can conclude that higher regional flortaucipir SUVR and lower regional cortical thickness additively contributed to lowest memory z-scores.

The role of global PIB SUVR levels is illustrated in Fig. 3 in which the entorhinal cortex flortaucipir SUVR × entorhinal cortex cortical thickness plots are stratified by three levels of global PIB SUVR. The PIB cut-points were chosen only for illustrative purposes. The main message in Fig. 3 was that worse memory z-scores occurred in the two strata with higher global PIB SUVR, and the lowest memory z-scores were seen with the highest global PIB SUVR, highest entorhinal cortex flortaucipir SUVR and lowest entorhinal cortex cortical thickness.

We also examined the continuous relationships of global PIB SUVR to memory z-scores in relation to entorhinal cortex flortaucipir SUVR (Fig. 4A) and to entorhinal cortex cortical thickness (Fig. 4B). In these heat maps, the transition zone for declining memory z-scores was in the range of 2.0 to 2.3 for global PIB SUVR. Elevated flortaucipir SUVR or low cortical thickness were associated with lower memory z-scores across all levels of PIB SUVR, but only at high PIB SUVR were the lowest memory z-scores seen. The other four regions show relationships between memory z-score and PIB SUVR versus flortaucipir SUVR and PIB SUVR versus cortical thickness that followed the same pattern as entorhinal cortex but were attenuated (Supplementary Fig. 5).

When we examined models using entorhinal cortex PIB SUVR rather than global PIB SUVR (Fig. 5), we found that the relationship of memory z-score to regional entorhinal cortex PIB SUVR versus flortaucipir SUVR (Fig. 5B) was substantially attenuated compared to global PIB (*cf.* Fig. 4A). Substituting regional for global PIB SUVR had no impact on associations between flortaucipir SUVR and cortical thickness and memory z-score.

In Fig. 6, we show the GBM-generated bivariate curves depicting the distributions of entorhinal cortex cortical thickness, entorhinal cortex flortaucipir SUVR and global PIB SUVR versus memory z-scores. These curves summarize the relationship of the biomarker to memory z-scores after accounting for all other variables. The bivariate curves

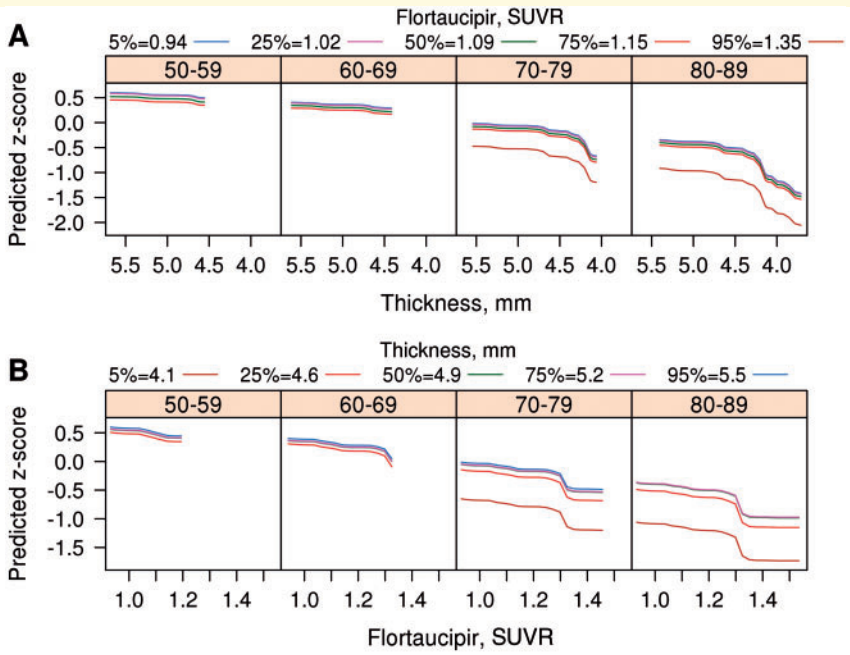

Figure 2 2D renderings of relationships of flortaucipir SUVR, cortical thickness and memory z-scores for entorhinal cortex. Predicted memory z-score is shown on the *y*-axis, while (**A**) cortical thickness (inverted scale) and (**B**) flortaucipir SUVR are on the *x*-axis. A family of curves is shown in colour code that represents: (**A**) different levels of flortaucipir SUVR and (**B**) cortical thickness. These two sets of graphs represent in 2D that which is depicted in Fig. 1A in 3D. As with the heat maps, the ranges for depicted values were set at the 3rd and 97th percentiles of the distribution of each biomarker by decade of age.

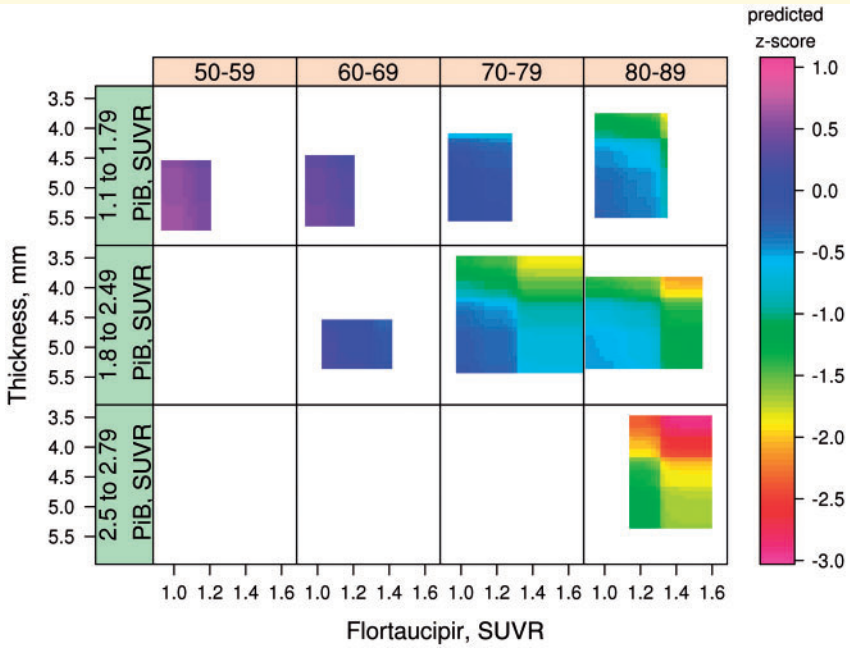

Figure 3 3D heat maps generated by GBM for entorhinal cortex broken down by three levels of global PIB SUVR. For each, four age ranges are represented: 50–59, 60–69, 70–79 and 80–89 years. Flortaucipir SUVR is on the *x*-axis, Cortical thickness on the *y*-axis (inverted scale) and predicted memory z-score on the *z*-axis as depicted by the colour code for each individual graph. Heat map ranges were set at the 3rd and 97th percentiles of the distribution of each biomarker by decade of age. The main finding illustrated is that the lowest memory performance, as indicated on the heat map occurred with the lowest levels of cortical thickness, the highest levels of flortaucipir SUVR in the setting of PIB SUVR $>$ 1.8. Also illustrated here is the relationship between global PIB SUVR and the distributions of entorhinal cortex flortaucipir SUVR and entorhinal cortex cortical thickness. Flortaucipir SUVR $>$ 1.4 was not seen in the lowest global PIB SUVR strata, and very low flortaucipir SUVR was infrequent in the highest global PIB SUVR strata. Similarly, while all levels of cortical thickness were seen in the lowest two global PIB SUVR strata, very thick entorhinal cortex cortical thickness levels were infrequent in the highest global PIB SUVR strata.

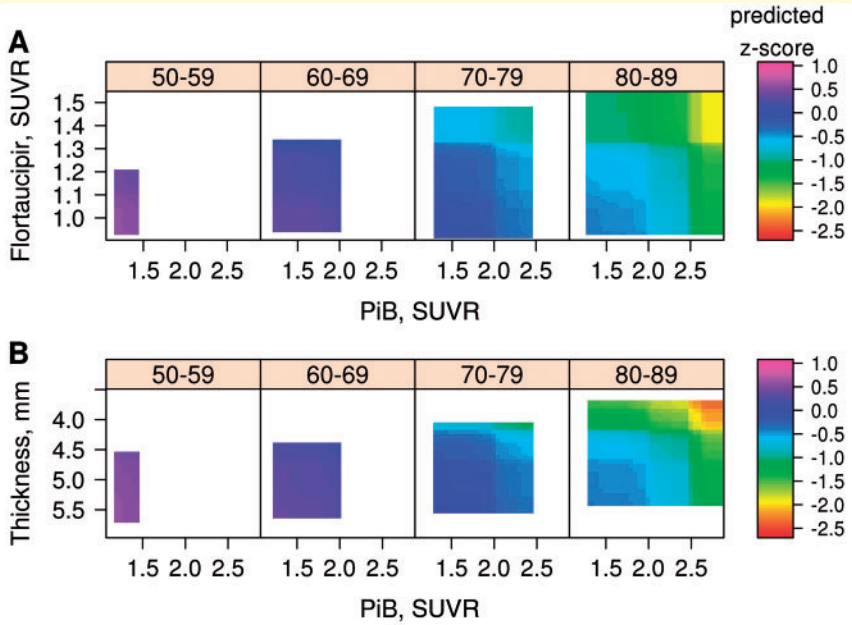

Figure 4 3D heat maps generated by GBM for entorhinal cortex. (**A**) Global PIB SUVR versus flortaucipir SUVR; and (**B**) global PIB SUVR versus cortical thickness. For each, four age ranges are represented: 50–59, 60–69, 70–79 and 80–89 years. Global PIB SUVR is on the *x*-axis in **A** and **B**. In **A**, flortaucipir SUVR is on the *y*-axis, and in **B**, cortical thickness (inverted scale) is on the *y*-axis. Predicted memory z-scores are represented on the z-axis as depicted by the colour code for each individual graph. The heat maps' ranges were set at the 3rd and 97th percentiles of the distribution of each biomarker by decade of age. The third pairing of biomarker—entorhinal cortex flortaucipir SUVR versus cortical thickness—heat map is found in Fig. 1A.

are shown on the same *x*-axis scale as the scatterplots for each biomarker for three groups: the 50–59-year-old group, the rest of the participants aged 60+ years, and patients with Alzheimer's disease dementia with elevated global PIB SUVR. The relationship between the segment ('critical' segment) of the biomarker values in which memory z-score declines were steepest differed for the three biomarkers. The 50–59-year-old group represents an age range in which elevations in PIB and flortaucipir SUVRs are infrequent. The critical segment for entorhinal cortex cortical thickness began at the top quartile among the 60+-year-olds but included the entire range of the Alzheimer's disease dementia group. For entorhinal cortex flortaucipir SUVR, the critical segment was beyond that seen in the 50–59-year-olds but was far short of that seen in the Alzheimer's disease dementia group. The critical segment for global PIB SUVR, on the other hand, was further to the right including only a region well into the upper quartile of the 60+-year-old group and within the Alzheimer's disease dementia range.

We performed sensitivity analyses in which we examined global z-scores rather than memory z-scores as the outcome to be predicted (Supplementary Fig. 6). We saw similar, though attenuated, relationships in the entorhinal cortex and other regions between global z-scores and the biomarkers compared to memory z-scores, as one would expect given the prominent clinical-anatomic relationships between memory performance and entorhinal cortex. Finally, we also examined models that were limited to cognitively unimpaired participants. Although the range of low memory z-scores was more limited, the same relationships were evident between biomarkers and cognition (Supplementary Fig. 7).

Discussion

We used a machine learning algorithm to model memory performance in non-demented individuals as a simultaneous function of PIB SUVR, flortaucipir SUVR and cortical thickness. Other than our prior analysis (Knopman *et al.*, 2018) that was restricted to global PIB SUVR and a meta-region of interest for cortical thickness, we are not aware of other explorations of the continuous distributions of PIB SUVR, flortaucipir SUVR and cortical thickness considered jointly. There were four principal findings: (i) in this population-based study, associations between biomarkers and memory z-score were strongly age-related; (ii) the entorhinal cortex showed the strongest relationships between memory z-scores, flortaucipir SUVR and cortical thickness; (iii) all three biomarkers were independently associated (additive) with memory z-scores; and (iv) each biomarker had a characteristic quantitative relationship to memory z-scores. Our analyses provide a unique view of the roles and responsibilities of each of the biomarkers during the non-demented phase of the Alzheimer process.

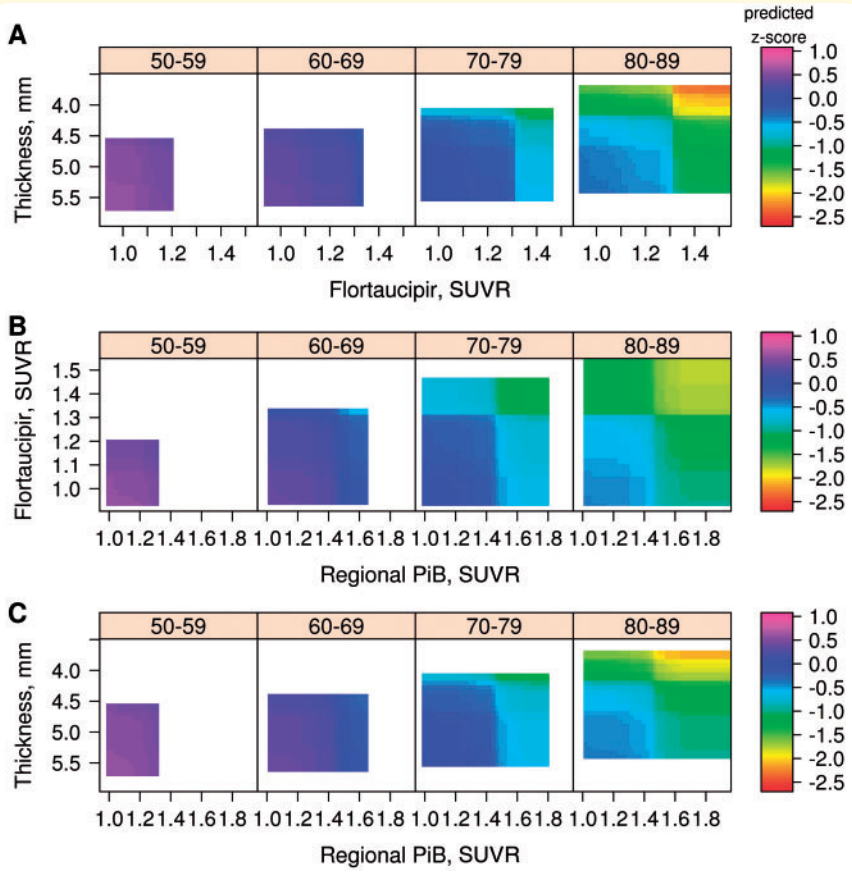

Figure 5 3D heat maps generated by GBM for entorhinal cortex. (**A**) Flortaucipir SUVR versus cortical thickness (inverted scale); (**B**) regional (entorhinal) PIB SUVR versus flortaucipir SUVR; and (**C**) regional (entorhinal) PIB SUVR versus cortical thickness. For each, four age ranges are represented: 50–59, 60–69, 70–79 and 80–89 years. Predicted memory z-scores are represented on the z-axis as depicted by the colour code for each individual graph. Heat map ranges were set at the 3rd and 97th percentiles of the distribution of each biomarker. The flortaucipir SUVR versus cortical thickness heat map (**A**) was similar to that seen (Fig. 1A) when global PIB SUVR was in the model. The entorhinal cortex regional PIB SUVR versus cortical thickness heat map (**C**) was also similar to that seen (Fig. 4B) with global PIB. However, the heat map of regional PIB SUVR versus regional flortaucipir showed a much attenuated relationship with PIB SUVR compared to the heat map with global PIB SUVR (Fig. 4A), suggesting that entorhinal cortex PIB SUVR and flortaucipir SUVR share more variance than do global PIB SUVR and entorhinal cortex flortaucipir SUVR.

The relationship of entorhinal cortex flortaucipir to memory function

Flortaucipir SUVR elevations in entorhinal cortex, in the presence of low cortical thickness, were associated with declining memory function when flortaucipir signal was above background. Elevations of flortaucipir SUVR in the entorhinal cortex were highly relevant to memory function, consistent with our expectations based on findings from multiple sources. From the neuropathology of tauopathy in Alzheimer's disease (Arnold *et al.*, 1991; Braak *et al.*, 1991; Arriagada *et al.*, 1992; Ingelsson *et al.*, 2004) to the repeated structural MRI observations of associations of hippocampal volume with memory functioning (Jack *et al.*, 1997; Killiany *et al.*, 2000) and risk for future dementia (Jack *et al.*, 1999), as well as more recent work with flortaucipir (Lowe *et al.*, submitted for publication), the medial temporal lobe is the anatomic substrate for both changes in memory functioning with ageing and with histopathology of Alzheimer's disease.

We show here that those who had elevated PIB SUVRs had higher mean flortaucipir SUVR, replicating the observations of others that elevated regional flortaucipir SUVR is contingent on the presence of elevated global PIB SUVR (Johnson *et al.*, 2015; Brier *et al.*, 2016; Cho *et al.*, 2016; Ossenkoppele *et al.*, 2016; Scholl *et al.*, 2016; Schwarz *et al.*, 2016; Marks *et al.*, 2017; Pontecorvo *et al.*, 2017; Leal *et al.*, 2018) particularly in the entorhinal cortex (Vemuri *et al.*, 2017). Although medial temporal tauopathy can occur in the absence of β-amyloidosis (Duyckaerts *et al.*, 1997; Price *et al.*, 1999), elevated β-amyloidosis facilitates 3R/4R tau burden and anatomic extent. This relationship is entirely consistent with neuropathological observations of the contingent relationship of elevated tauopathy on β-amyloidosis (Nelson *et al.*, 2007; Hyman *et al.*, 2012).

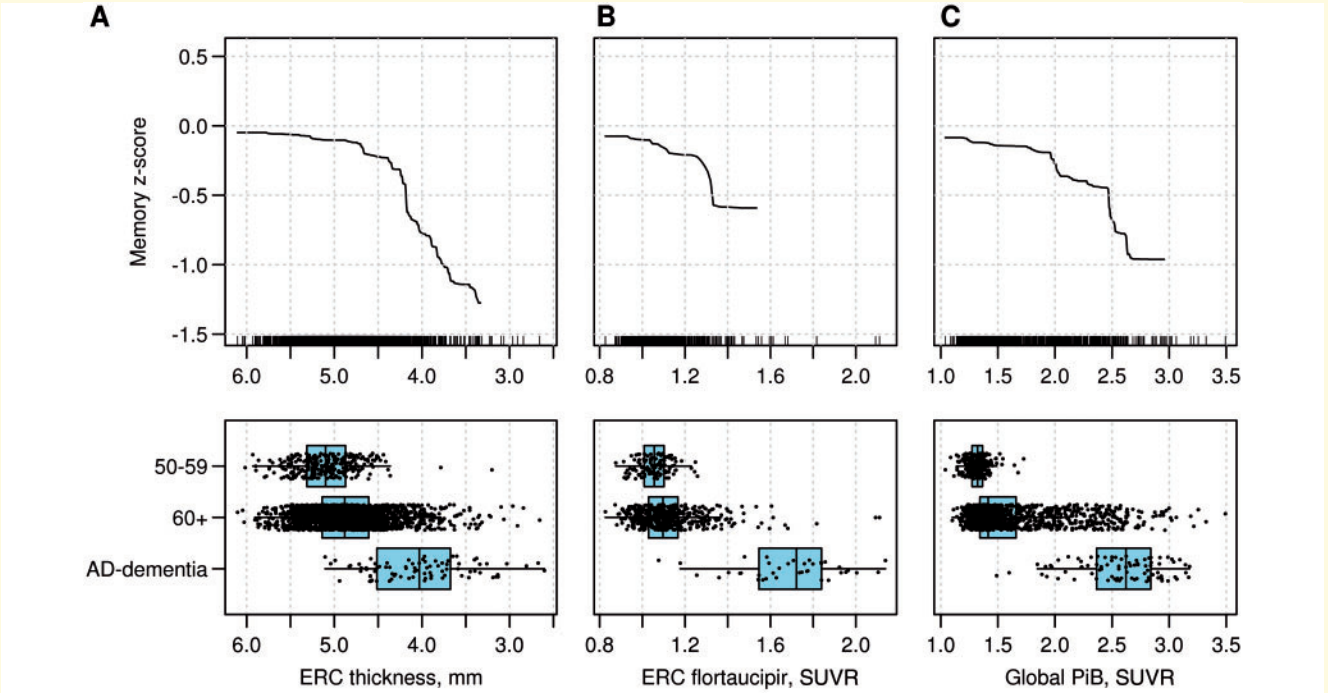

Figure 6 The bivariate relationships between each biomarker. (**A**) Entorhinal cortical thickness (inverted scale); (**B**) Entorhinal flortaucipir SUVR; and (**C**) global PIB SUVR and predicted memory z-score (*y*-axis) are shown on the *top row*. The curves are right-truncated at the 10th smallest or 10th largest of the distribution of each biomarker. The *y*-axis values for memory z-scores range from +0.5 to −1.5. The small vertical lines on the *x*-axis each represent individual participants. In the *bottom row* are shown scatterplots of the distribution for biomarkers in three groups: cognitively unimpaired participants between the ages of 50 and 59 years, non-demented participants 60 years and older; and subjects with Alzheimer's disease (AD) dementia ($n = 83$) from the Mayo Clinic Alzheimer's Disease Research Center and MCSA. The latter group was not included in GBM modelling and is shown here for comparison purposes. The figure shows the relationships of the 'critical segments' of each biomarker's range (i.e. the range where memory z-scores show the greatest decline in non-demented study participants). ERC = entorhinal cortex.

The relationship of entorhinal cortex cortical thickness to memory function

In the current study, low entorhinal cortex cortical thickness was associated with lower memory z-scores despite inclusion of age, flortaucipir or PIB SUVRs in the model. In fact, low entorhinal cortex cortical thickness appeared necessary for low memory z-scores. The current results replicate our previous work (Knopman *et al.*, 2018) on relationships of cortical thickness to cognition, even though we used a much smaller region of interest and focused on memory currently. Even with low flortaucipir SUVR, low entorhinal cortex cortical thickness was associated with some decline in memory z-scores. Cortical thickness is a reasonable proxy for neuronal cell loss and synapse loss (DeKosky *et al.*, 1990; Terry *et al.*, 1991; Gomez-Isla *et al.*, 1997; Giannakopoulos *et al.*, 2003; Scheff *et al.*, 2007; Savva *et al.*, 2009; Andrade-Moraes *et al.*, 2013), and generally in the neuropathology literature, structural integrity measures show a stronger relationship to cognitive status than tauopathy.

Cortical thickness in the entorhinal cortex in non-demented subjects may be modestly associated with entorhinal cortex flortaucipir as seen here in our oldest subgroup (Supplementary Fig. 3D) and as reported by others (Sepulcre *et al.*, 2016). Importantly, elevated flortaucipir SUVR in medial temporal structures is associated with worsening atrophy (Das *et al.*, 2018). Amyloid-β burden is also associated with volume loss in the medial temporal lobe. In prior studies using categorical classifications in which we lacked flortaucipir imaging, there was a weak association of PIB SUVR on hippocampal volume but stronger associations with changes in hippocampal volume (Knopman *et al.*, 2013, Petersen *et al.*, 2015). In the current cross-sectional studies we cannot claim that cortical thickness was under the influence of tauopathy and β-amyloidosis, but we believe we are on firm ground in hypothesizing that such links exist. However, the cross-sectional data are clear that neither rising PIB SUVR nor flortaucipir SUVR have an exclusive control over cortical thickness.

Cortical thickness is affected by many processes other than tauopathy and β-amyloidosis that compromise cortical integrity over a lifetime, including genetic (Brouwer *et al.*, 2017), childhood nutritional and educational (EClipSE Collaborative Members *et al.*, 2010; Kim *et al.*, 2015) factors, and acquired insults to the brain, such as trauma, vascular risk factors (Leritz *et al.*, 2011) or other systemic

conditions (Driscoll *et al.*, 2009; Nelson *et al.*, 2011; Crivello *et al.*, 2014; Fjell *et al.*, 2014). The level of cortical thickness that exists at the time point that flortaucipir SUVR rises above background will vary greatly from person to person. Because we found that the level of entorhinal cortex cortical thickness had a major modifying effect on the cognitive consequences of the pathological elevations of flortaucipir and PIB SUVRs, entorhinal cortex cortical thickness represents a biomarker that could be downstream of β-amyloidosis and tauopathic neurodegeneration, and is also a proxy for brain reserve. In fact, the two concepts are inextricably linked. A protective effect of larger temporal lobe volume on memory function in the presence of elevated amyloid-β has been seen by others (Chetelat *et al.*, 2010). Further studies of the relationship between tauopathy and cortical structural integrity are needed, but we would assert that the interplay between cortical thickness and tauopathy is one explanation for the large degree of variability in the impact of tauopathy on memory.

The relationship of PIB SUVR to memory function

Global PIB SUVR was associated with low memory z-score to a slight degree at levels just above background PIB SUVR, but the level at which global PIB SUVR was associated with steeply lower memory z-scores was at its highest range as occurs in subjects with dementia. With flortaucipir SUVR in the current model, in contrast to our prior work (Knopman *et al.*, 2018), associations between memory z-scores and PIB SUVR were modest at lower PIB SUVR levels. This latter association was weaker still when regional entorhinal cortex PIB SUVR was substituted in the model, suggesting it was not local amyloid-β accumulation that was critical. Regions other than the medial temporal lobe are where early amyloid-β accumulation occurs (Gonneaud *et al.*, 2017; Palmqvist *et al.*, 2017). The lag of 20–30 years between the initiation of amyloid-β elevations and achieving the magnitude of PIB SUVR in which we observed the steep declines in memory z-scores (Rowe *et al.*, 2010; Villemagne *et al.*, 2013) suggests that rising PIB SUVR, even to levels considered abnormal, is dissociated from cognition. To account for the association between elevated global PIB and memory z-scores, we therefore conjecture that global PIB SUVR functions as a marker of duration of other pathological processes of Alzheimer's disease that become active 20–30 years into amyloid-β accumulation. That conjecture would allow us to account for the persistence of the association of high global PIB SUVR and memory z-scores, by asserting that high PIB is a measure of pathology in the Alzheimer's disease pathway not accounted for by entorhinal cortex flortaucipir or cortical thickness. For example, elevated global PIB SUVR, more so than regional PIB, could be a proxy for worsening network disruption (Jones *et al.*, 2017).

Other cortical regions

Flortaucipir SUVR and cortical thickness were also related to memory z-scores in parahippocampal gyrus and inferior temporal gyrus, but associations were not as strong as in entorhinal cortex. As expected, imaging biomarkers in posterior cingulate and the prefrontal region of interest showed very little association with memory z-scores. We also examined other regions, but as most regions outside of the medial temporal lobe have little tau in non-demented subjects (Lowe *et al.*, 2018), we would not have expected to see flortaucipir SUVR × memory z-score associations.

In the current analyses, we have viewed each region independently, except for β-amyloidosis, thereby ignoring any effects of regional connectivity. Fully integrating more relevant biomarkers and accounting for interplay between regions is clearly a major computational challenge the field needs to address.

The influence of age

Age played a large role on cognition in this population-based sample of non-demented people. The extent to which age remained associated with memory z-scores in our modelling demonstrates that there is much variance yet to be explained after accounting for PIB, flortaucipir and cortical thickness. As most patients dying with Alzheimer's disease also have other pathologies (Schneider *et al.*, 2009; Robinson *et al.*, 2018), we believe that age effects could eventually be accounted for by defined disease conditions (Power *et al.*, 2018). However, it was well beyond the scope of the current analyses to incorporate biomarkers of cerebrovascular disease, which may the most commonly coexisting of the age-related pathologies that we know about (Arvanitakis *et al.*, 2016). In the future, accounting for α-synucleinopathy or TDP43 proteinopathy will also have to be addressed. However, given the high dimensionality of our current models, adding additional biomarkers will require additional computational and graphic sophistication.

Strengths and limitations

Strengths of the current analysis include the large, well characterized cohort of non-demented individuals who had all three imaging biomarkers. In addition, the GBM approach offered a flexible method for analysing multidimensional data. There are also limitations to our studies. Although the participants were drawn from a population-based study and all eligible participants were invited to undergo brain imaging, we do not know whether the imaging features of current cohort differed systematically from those MCSA participants who did not undergo imaging. The current study was cross-sectional, thereby limiting

any predictive analyses. Although there is evidence that both PIB SUVR (Murray *et al.*, 2015) and flortaucipir SUVR (Alzforum, 2018) are correlated with their neuropathological counterparts, it may be premature to equate the PET biomarkers with amyloid-β and Alzheimer's disease tauopathy. Associations between flortaucipir and cognition may be understated because flortaucipir is known to be associated with nonspecific binding to iron, monoamine oxidase enzymes, to 4-repeat tau and to an unknown receptor in relation to TDP-43. Cross-sectional biomarker observations cannot be used to make definitive statements about causal links between amyloid-β, 3R/4R tauopathy and cortical neuronal integrity. Biomarkers are not the actual biological actors; hence one should approach inferences about treatment targets from these observations with caution. The use of the GBM modelling enabled us to examine relationships among imaging biomarkers without prespecifying their functional form. While we were able to replicate our prior studies that used only amyloid-β and cortical thickness biomarkers, we found that we were able to take our analyses down to smaller more functionally homogeneous regions.

Conclusion

We can draw some inferences about the sequence of appearance of the biomarker changes in relation to cognition up to the onset of overt cognitive impairment. As cortical thickness in late life represents the sum of a lifetime of acquired pathologies, lower cortical thickness is under multiple influences besides β-amyloidosis and tauopathy. It was only at very elevated levels of PIB SUVR (entorhinal cortex or global) that we saw associations with low memory scores, consistent with the view that β-amyloidosis is not a proximal influence on cognition. Brain amyloid-β levels are better considered as a proxy for the duration of a neurodegenerative process, and as a necessary precondition for elevated flortaucipir SUVR. Flortaucipir SUVR elevation above background was closely associated with lower memory performance. Dysfunction of processes involved in learning and delayed recall are substantially influenced by the confluence of amyloid-β-enabled elevations of entorhinal cortex tauopathy and lower levels of entorhinal cortex cortical thickness.

Acknowledgements

We gratefully acknowledge the contributions of our participants, and our staff at the Mayo Alzheimer Center for their invaluable contributions to this work. We would like to greatly thank AVID Radiopharmaceuticals, Inc., for their support in supplying AV-1451 precursor, chemistry production advice and oversight, and FDA regulatory cross-filing permission and documentation needed for this work.

Funding

This work was supported by NIH grants P50 AG16574, U01 AG06786, R01 AG034676, R01 AG41851, and R37 AG11378, the Elsie and Marvin Dekelboum Family Foundation, the Robert H. and Clarice Smith and Abigail Van Buren Alzheimer's Disease Research Program of the Mayo Foundation, GHR Foundation, Alexander Family Alzheimer's Disease Research Professorship of the Mayo Clinic, a Liston Award, Schuler Foundation and the Mayo Foundation for Medical Education and Research.

Competing interests

D.S.K. serves on a Data Safety Monitoring Board for the DIAN study; is an investigator in clinical trials sponsored by Biogen, Lilly Pharmaceuticals and the University of Southern California; and receives research support from the NIH. C.R.J. receives research support from the NIH/NIA, and the Alexander Family Alzheimer's Disease Research Professorship of the Mayo Foundation. P.V. receives research grants from the NIH/NIA. M.M.Mi. served as a consultant to Eli Lilly and Lysosomal Therapeutics, Inc. She receives research support from the National Institutes of Health (R01 AG49704, P50 AG44170, U01 AG06786, RF1 AG55151), Department of Defense (W81XWH-15–1), and unrestricted research grants from Biogen, Roche, and Lundbeck. M.M.Ma. receives research support from the NIH/NIA & NIDCD. V.J.L. serves on scientific advisory boards for Bayer Schering Pharma, Merck Research, Piramal Life Sciences and receives research support from GE Healthcare, Siemens Molecular Imaging, AVID Radiopharmaceuticals and the NIH (NIA, NCI) K.K. receives research grants from the NIH/NIA. J.G-R. reports no disclosures. He receives research grants from the NIH/NIA. B.F.B. has served as an investigator for clinical trials sponsored by GE Healthcare, FORUM Pharmaceuticals, C2N Diagnostics and Axovant. He receives publishing royalties Behavioral Neurology Of Dementia (Cambridge Medicine, 2009, 2016). He serves on the Scientific Advisory Board of the Tau Consortium. He receives research support from the NIH, the Mayo Clinic Dorothy, Harry T. Mangurian Jr. Lewy Body Dementia Program and the Little Family Foundation. T.M.T. receives research grants from the NIH. R.C.P. serves on data monitoring committees for Janssen Alzheimer Immunotherapy, and is a consultant for Biogen, Roche, Merck, Genentech, Inc; receives publishing royalties from Mild Cognitive Impairment (Oxford University Press, 2003), and receives research support from the NIH/NIA. J.L.G., M.L.S., D.T.J., C.G.S., and E.S.L. report no disclosures.

Supplementary material

Supplementary material is available at *Brain* online.

References

Alzforum. It's Official: Tau PET Sees Tangles, and Staging Tangles Predicts Decline [Internet]. 2018. [cited 2018 Oct 1] Available from: https://www.alzforum.org/news/conference-coverage/its-official-tau-pet-sees-tangles-and-staging-tangles-predicts-decline.

Andrade-Moraes CH, Oliveira-Pinto AV, Castro-Fonseca E, da Silva CG, Guimaraes DM, Szczupak D, et al. Cell number changes in Alzheimer's disease relate to dementia, not to plaques and tangles. Brain 2013; 136: 3738–52.

Arnold SE, Hyman BT, Flory J, Damasio AR,Van Hoesen GW. The topographical and neuroanatomical distribution of neurofibrillary tangles and neuritic plaques in the cerebral cortex of patients with Alzheimer's disease. Cereb Cortex 1991; 1: 103–16.

Arriagada PV, Growdon JH, Hedley-Whyte ET, Hyman BT. Neurofibrillary tangles but not senile plaques parallel duration and severity of Alzheimer's disease. Neurology 1992; 42: 631–9.

Arvanitakis Z, Capuano AW, Leurgans SE, Bennett DA, Schneider JA. Relation of cerebral vessel disease to Alzheimer's disease dementia and cognitive function in elderly people: a cross-sectional study. Lancet Neurol 2016; 15: 934–43.

Ashburner J, Friston KJ. Unified segmentation. Neuroimage 2005; 26: 839–51.

Avants BB, Epstein CL, Grossman M, Gee JC. Symmetric diffeomorphic image registration with cross-correlation: evaluating automated labeling of elderly and neurodegenerative brain. Med Image Anal 2008; 12: 26–41.

Bilgel M, An Y, Helphrey J, Elkins W, Gomez G, Wong DF, et al. Effects of amyloid pathology and neurodegeneration on cognitive change in cognitively normal adults. Brain 2018; 8: 2475–85.

Braak H, Braak E. Neuropathological staging of Alzheimer-related changes. Acta Neuropathol (Berl) 1991; 82: 239–59.

Brier MR, Gordon B, Friedrichsen K, McCarthy J, Stern A, Christensen J, et al. Tau and Abeta imaging, CSF measures, and cognition in Alzheimer's disease. Sci Transl Med 2016; 8: 338ra366.

Brouwer RM, Panizzon MS, Glahn DC, Hibar DP, Hua X, Jahanshad N, et al. Genetic influences on individual differences in longitudinal changes in global and subcortical brain volumes: results of the ENIGMA plasticity working group. Hum Brain Mapp. 2017; 38: 4444–58.

Burnham SC, Bourgeat P, Dore V, Savage G, Brown B, Laws S, et al. Clinical and cognitive trajectories in cognitively healthy elderly individuals with suspected non-Alzheimer's disease pathophysiology (SNAP) or Alzheimer's disease pathology: a longitudinal study. Lancet Neurol 2016; 15: 1044–53.

Chetelat G, Villemagne VL, Pike KE, Baron JC, Bourgeat P, Jones G, et al. Larger temporal volume in elderly with high versus low beta-amyloid deposition. Brain 2010; 133: 3349–58.

Cho H, Choi JY, Hwang MS, Kim YJ, Lee HM, Lee HS, et al. In vivo cortical spreading pattern of tau and amyloid in the Alzheimer disease spectrum. Ann Neurol 2016; 80: 247–58.

Crivello F, Tzourio-Mazoyer N, Tzourio C,Mazoyer B. Longitudinal assessment of global and regional rate of grey matter atrophy in 1,172 healthy older adults: modulation by sex and age. PLoS One 2014; 9: e114478.

Das SR, Avants BB, Grossman M, Gee JC. Registration based cortical thickness measurement. Neuroimage 2009; 45: 867–79.

Das SR, Xie L, Wisse LEM, Ittyerah R, Tustison NJ, Dickerson BC, et al. Longitudinal and cross-sectional structural magnetic resonance imaging correlates of AV-1451 uptake. Neurobiol Aging 2018; 66: 49–58.

DeKosky ST, Scheff SW. Synapse loss in frontal cortex biopsies in Alzheimer's disease: correlation with cognitive severity. Ann Neurol 1990; 27: 457–64.

Driscoll I, Davatzikos C, An Y, Wu X, Shen D, Kraut M, et al. Longitudinal pattern of regional brain volume change differentiates normal aging from MCI. Neurology 2009; 72: 1906–13.

Duyckaerts C, Hauw JJ. Prevalence, incidence and duration of Braak's stages in the general population: can we know? Neurobiol Aging 1997; 18: 362–9; discussion 389–392.

EClipSE Collaborative Members, Brayne C, Ince PG, Keage HA, McKeith IG, Matthews FE, et al. Education, the brain and dementia: neuroprotection or compensation? Brain 2010; 133: 2210–6.

Fjell AM, Westlye LT, Grydeland H, Amlien I, Espeseth T, Reinvang I, et al. Accelerating cortical thinning: unique to dementia or universal in aging? Cereb Cortex 2014; 24: 919–34.

Giannakopoulos P, Herrmann FR, Bussiere T, Bouras C, Kovari E, Perl DP, et al. Tangle and neuron numbers, but not amyloid load, predict cognitive status in Alzheimer's disease. Neurology 2003; 60: 1495–500.

Gomez-Isla T, Hollister R, West H, Mui S, Growdon JH, Petersen RC, et al. Neuronal loss correlates with but exceeds neurofibrillary tangles in Alzheimer's disease. Ann Neurol 1997; 41: 17–24.

Gonneaud J, Arenaza-Urquijo EM, Mezenge F, Landeau B, Gaubert M, Bejanin A, et al. Increased florbetapir binding in the temporal neocortex from age 20 to 60 years. Neurology 2017; 89: 2438–46.

Grothe MJ, Barthel H, Sepulcre J, Dyrba M, Sabri O, Teipel SJ. In vivo staging of regional amyloid deposition. Neurology 2017; 89: 2031–8.

Hyman BT, Phelps CH, Beach TG, Bigio EH, Cairns NJ, Carrillo MC, et al. National Institute on Aging-Alzheimer's Association guidelines for the neuropathologic assessment of Alzheimer's disease. Alzheimers Dement 2012; 8: 1–13.

Ingelsson M, Fukumoto H, Newell KL, Growdon JH, Hedley-Whyte ET, Frosch MP, et al. Early Abeta accumulation and progressive synaptic loss, gliosis, and tangle formation in AD brain. Neurology 2004; 62: 925–31.

Jack CR Jr, Knopman DS, Chetelat G, Dickson D, Fagan AM, Frisoni GB, et al. Suspected non-Alzheimer disease pathophysiology - concept and controversy. Nat Rev Neurol 2016; 12: 117–24.

Jack CR Jr, Lowe VJ, Senjem ML, Weigand SD, Kemp BJ, Shiung MM, et al. 11C PiB and structural MRI provide complementary information in imaging of Alzheimer's disease and amnestic mild cognitive impairment. Brain. 2008; 131: 665–80.

Jack CR Jr., Petersen RC, Xu YC, Waring SC, O'Brien PC, Tangalos EG, et al. Medial temporal atrophy on MRI in normal aging and very mild Alzheimer's disease. Neurology 1997; 49: 786–94.

Jack CR Jr., Wiste HJ, Schwarz CG, Lowe VJ, Senjem ML, Vemuri P, et al. Longitudinal tau PET in ageing and Alzheimer's disease. Brain 2018; 141: 1517–28.

Jack CR, Petersen RC, Xu YC, O'Brien PC, Smith GE, Ivnik RJ, et al. Prediction of AD with MRI-based hippocampal volume in mild cognitive impairment. Neurology 1999; 52: 1397–403.

Jack CR, Wiste HJ, Weigand SD, Therneau TM, Lowe VJ, Knopman DS, et al. Defining imaging biomarker cut-points for brain aging and Alzheimer's disease. Alzheimer's Dementia 2017; 13: 205–16.

Johnson KA, Schultz A, Betensky RA, Becker JA, Sepulcre J, Rentz D, et al. Tau PET imaging in aging and early Alzheimer's disease. Ann Neurol 2015; 79: 110–9.

Jones DT, Graff-Radford J, Lowe VJ, Wiste HJ, Gunter JL, Senjem ML, et al. Tau, amyloid, and cascading network failure across the Alzheimer's disease spectrum. Cortex 2017; 97: 143–59.

Killiany RJ, Gomez-Isla T, Moss M, Kikinis R, Sandor T, Jolesz F, et al. Use of structural magnetic resonance imaging to predict who will get Alzheimer's disease. Ann Neurol 2000; 47: 430–9.

Kim JP, Seo SW, Shin HY, Ye BS, Yang JJ, Kim C, et al. Effects of education on aging-related cortical thinning among cognitively normal individuals. Neurology 2015; 85: 806–12.

Knopman DS, Beiser A, Machulda MM, Fields J, Roberts RO, Pankratz VS, et al. Spectrum of cognition short of dementia: Framingham Heart Study and Mayo Clinic Study of Aging. Neurology 2015; 85: 1712–21.

Knopman DS, Jack CRJ, Wiste HJ, Weigand SD, Vemuri P, Lowe VJ, et al. Selective worsening of brain injury biomarker abnormalities in cognitively normal elderly with β-amyloidosis. JAMA Neurol 2013; 70: 1030–8.

Knopman DS, Lundt ES, Therneau TM, Vemuri P, Lowe VJ, Kantarci K, et al. Joint associations of beta-amyloidosis and cortical thickness with cognition. Neurobiol Aging 2018; 65: 121–31.

Leal SL, Lockhart SN, Maass A, Bell RK,Jagust WJ. Subthreshold amyloid predicts tau deposition in aging. J Neurosci 2018; 38: 4482–9.

Leritz EC, Salat DH, Williams VJ, Schnyer DM, Rudolph JL, Lipsitz L, et al. Thickness of the human cerebral cortex is associated with metrics of cerebrovascular health in a normative sample of community dwelling older adults. Neuroimage 2011; 54: 2659–71.

Lockhart SN, Scholl M, Baker SL, Ayakta N, Swinnerton KN, Bell RK, et al. Amyloid and tau PET demonstrate region-specific associations in normal older people. Neuroimage 2017; 150: 191–9.

Lowe VJ, Bruinsma T, Wiste H, Min HK, Fang P, Senjem ML, et al. Cross-sectional associations of Tau-PET signal with cognition in cognitively unimpaired adults. Neurology, submitted for publication.

Lowe VJ, Bruinsma TJ, Min HK, Lundt ES, Fang P, Senjem ML, et al. Elevated medial temporal lobe and pervasive brain tau-PET signal in normal participants. Alzheimers Dement (Amst) 2018; 10: 210–6.

Lowe VJ, Wiste HJ, Senjem ML, Weigand SD, Therneau TM, Boeve BF, et al. Widespread brain tau and its association with ageing, Braak stage and Alzheimer's dementia. Brain 2018; 141: 271–87.

Marks SM, Lockhart SN, Baker SL, Jagust WJ. Tau and beta-amyloid are associated with medial temporal lobe structure, function, and memory encoding in normal aging. J Neurosci 2017; 37: 3192–201.

Murray ME, Lowe VJ, Graff-Radford NR, Liesinger AM, Cannon A, Przybelski SA, et al. Clinicopathologic and 11C-Pittsburgh compound B implications of Thal amyloid phase across the Alzheimer's disease spectrum. Brain 2015; 138: 1370–81.

Nelson PT, Head E, Schmitt FA, Davis PR, Neltner JH, Jicha GA, et al. Alzheimer's disease is not "brain aging": neuropathological, genetic, and epidemiological human studies. Acta Neuropathol 2011; 121: 571–87.

Nelson PT, Jicha GA, Schmitt FA, Liu H, Davis DG, Mendiondo MS, et al. Clinicopathologic correlations in a large Alzheimer disease center autopsy cohort: neuritic plaques and neurofibrillary tangles "do count" when staging disease severity. J Neuropathol Exp Neurol 2007; 66: 1136–46.

Ossenkoppele R, Schonhaut DR, Scholl M, Lockhart SN, Ayakta N, Baker SL, et al. Tau PET patterns mirror clinical and neuroanatomical variability in Alzheimer's disease. Brain 2016; 139: 1551–67.

Palmqvist S, Scholl M, Strandberg O, Mattsson N, Stomrud E, Zetterberg H, et al. Earliest accumulation of beta-amyloid occurs within the default-mode network and concurrently affects brain connectivity. Nat Commun 2017; 8: 1214. doi: 1210.1038/s41467–41017–01150-x.

Petersen RC. Mild cognitive impairment as a diagnostic entity. J Intern Med 2004; 256: 183–94.

Petersen RC, Roberts RO, Knopman DS, Geda YE, Cha RC, Pankratz VS, et al. Prevalence of mild cognitive impairment is higher in men than in women. The Mayo Clinic Study of Aging. Neurology 2010; 75: 889–97.

Petersen RC, Wiste HJ, Weigand SD, Rocca WA, Roberts RO, Mielke MM, et al. Association of elevated amyloid levels with cognition and biomarkers in cognitively normal people from the community. JAMA Neurol 2015; 73: 85–92.

Pontecorvo MJ, Devous MD, Sr., Navitsky M, Lu M, Salloway S, Schaerf FW, et al. Relationships between flortaucipir PET tau binding and amyloid burden, clinical diagnosis, age and cognition. Brain 2017; 140: 748–63.

Power MC, Mormino E, Soldan A, James BD, Yu L, Armstrong NM, et al. Combined neuropathological pathways account for age-related risk of dementia. Ann Neurol 2018; 84: 10–22.

Price JL,Morris JC. Tangles and plaques in nondemented aging and "preclinical" Alzheimer's disease. Ann Neurol 1999; 45: 358–68.

Roberts RO, Geda YE, Knopman D, Cha R, Pankratz VS, Boeve B, et al. The Mayo Clinic Study of Aging: design and sampling, participation, baseline measures and sample characteristics. Neuroepidemiology 2008; 30: 58–69.

Roberts RO, Geda YE, Knopman DS, Cha RH, Pankratz VS, Boeve BF, et al. The incidence of MCI differs by subtype and is higher in men: The Mayo Clinic Study of Aging. Neurology 2012; 78: 342–51.

Roberts RO, Knopman DS, Mielke MM, Cha RH, Pankratz VS, Christianson TJ, et al. Higher risk of progression to dementia in mild cognitive impairment cases who revert to normal. Neurology 2014; 82: 317–25.

Robinson JL, Lee EB, Xie SX, Rennert L, Suh E, Bredenberg C, et al. Neurodegenerative disease concomitant proteinopathies are prevalent, age-related and APOE4-associated. Brain 2018; 141: 2181–93.

Rowe CC, Ellis KA, Rimajova M, Bourgeat P, Pike KE, Jones G, et al. Amyloid imaging results from the Australian Imaging, Biomarkers and Lifestyle (AIBL) study of aging. Neurobiol Aging 2010; 31: 1275–83.

Savva GM, Wharton SB, Ince PG, Forster G, Matthews FE, Brayne C. Age, neuropathology, and dementia. N Engl J Med 2009; 360: 2302–9.

Scheff SW, Price DA, Schmitt FA, DeKosky ST, Mufson EJ. Synaptic alterations in CA1 in mild Alzheimer disease and mild cognitive impairment. Neurology 2007; 68: 1501–8.

Schneider JA, Arvanitakis Z, Leurgans SE,Bennett DA. The neuropathology of probable Alzheimer disease and mild cognitive impairment. Ann Neurol 2009; 66: 200–8.

Scholl M, Lockhart SN, Schonhaut DR, O'Neil JP, Janabi M, Ossenkoppele R, et al. PET imaging of tau deposition in the aging human brain. Neuron 2016; 89: 971–82.

Schwarz AJ, Yu P, Miller BB, Shcherbinin S, Dickson J, Navitsky M, et al. Regional profiles of the candidate tau PET ligand 18F-AV-1451 recapitulate key features of Braak histopathological stages. Brain 2016; 139: 1539–50.

Schwarz CG, Gunter JL, Ward CP, Vemuri P, Senjem ML, Wiste HJ, et al. The mayo clinic adult lifespan template: better quantification across the lifespan. Alzheimer's Dement 2017; 13: P792.

Schwarz CG, Gunter JL, Wiste HJ, Przybelski SA, Weigand SD, Ward CP, et al. A large scale comparison of cortical thickness and volume methods for measuring Alzheimer's disease severity. Neuroimage Clin 2016; 11: 802–12.

Sepulcre J, Schultz AP, Sabuncu M, Gomez-Isla T, Chhatwal J, Becker A, et al. In vivo tau, amyloid, and gray matter profiles in the aging brain. J Neurosci 2016; 36: 7364–74.

Terry RD, Masliah E, Salmon DP, Butters N, DeTeresa R, Hill R, et al. Physical basis of cognitive alterations in Alzheimer's disease: synapse loss is the major correlate of cognitive impairment. Ann Neurol 1991; 30: 572–80.

Vemuri P, Lowe VJ, Knopman DS, Senjem ML, Kemp BJ, Schwarz CG, et al. Tau-PET uptake: regional variation in average SUVR and impact of amyloid deposition. Alzheimers Dement (Amst) 2017; 6: 21–30.

Villemagne VL, Burnham S, Bourgeat P, Brown B, Ellis KA, Salvado O, et al. Amyloid beta deposition, neurodegeneration, and cognitive decline in sporadic Alzheimer's disease: a prospective cohort study. Lancet Neurol 2013; 12: 357–67.